Application of Cars Spectroscopy To the Detection of So2

Aldén, Marcus; Wendt, W

Published in:
Applied Spectroscopy

DOI:
10.1366/0003702884429823

1988

6. A. Hartford, D. A. Cremers, T. R. Loree, and G. P. Quigley, Los Alamos Report No. LA-UR-83-409 (1983).
7. D. A. Greenhalgh, R. Devonshire, I. S. Dring, J. Meads, and H. F. Boyson. Chem. Phys. Letts. **133,** 458 (1987).
8. D. A. Greenhalgh, in *Advances in Infrared and Raman Spectroscopy, Advances in Non-Linear Spectroscopy,* R. E. Hester and R. J. H. Clarke, Eds. (Wiley, London, 1988), Chap. 5, p. 193.
9. R. J. Hall and A. C. Eckbreth, *Laser Applications,* J. F. Ready and R. K. Erf, Eds. (Academic Press, New York, 1984), Vol. 5.
10. S. A. J. Druet and J.-P. E. Taran, Progress in Quantum Electronics **7,** 1 (1981).
11. D. A. Greenhalgh and W. A. England, AERE Harwell Report No. R10282 (1982).
12. D. A. Greenhalgh, Raman Spectrosc. **14,** 150 (1983).
13. A. C. Eckbreth, Appl. Opt. **18,** 3215 (1979).
14. P. R. Hammond, Opt. Comm. **29,** 331 (1979).
15. M. D. Levenson and J. J. Song, Phys. Rev. Lett. **36,** 189 (1976).
16. R. L. Farrow, R. P. Lucht, G. L. Clark, and R. E. Palmer, Appl. Opt. **24,** 2241 (1985).
17. W. A. England, J. M. Milne, S. N. Jenny, and D. A. Greenhalgh, Appl. Spectrosc. **38,** 867 (1984).

Application of CARS Spectroscopy to the Detection of SO_2

MARCUS ALDÉN* and WILHELM WENDT

Combustion Center (M.A.) and Department of Physics (W.W.), Lund Institute of Technology, P.O. Box 118, S-221 00 Lund, Sweden

Experiments have been performed to investigate the possibility of detecting low concentrations of SO_2 using CARS spectroscopy. The experiments were also aimed at high-temperature investigations both in a heated cell and in a flame. During the cell measurements it was clearly revealed that the temperature has a dramatic influence on the shape of the CARS spectra, indicating a good potential for thermometry using SO_2 and CARS spectroscopy.

Index Headings: **CARS; Flames; Sulphur dioxide; Spectroscopy.**

INTRODUCTION

During the past two decades, the energy crisis and the growing awareness of our serious environmental situation caused by air pollution have encouraged increased research in basic combustion. The aim of this research has thus been to achieve a deeper insight into the phenomena which will ultimately increase the efficiency in industrial combustion processes at the same time that the emission of air pollutants is decreased. One of the key issues in understanding these phenomena is the use of nonintrusive diagnostic techniques, e.g., those utilizing lasers which give high spatial and temporal resolution.

Since the first demonstration of the application of laser techniques to combustion diagnostics—about twenty years ago—several techniques have emerged. For comprehensive reviews see, for example, Refs. 1–3. The technique which probably has the largest potential, at least in the practical sphere of measurements, is Coherent Anti-Stokes Raman Scattering, or CARS. Thanks to pioneering work by Taran and co-workers, the technique was introduced for studies of combustion phenomena in the early seventies.[4,5] After these first demonstrations, the technique was extended to allow it to yield both high temporal and spatial resolution measurements, through the introduction of the broad-band CARS[6] and the BOXCARS[7] techniques, respectively. During the past decade CARS has been used in numerous combustion applications, including sooty flames,[8] internal combustion engines,[9] and large-scale furnaces.[10,11] CARS has mostly been utilized for temperature measurements using the temperature dependence of the spectra. Since N_2 is the most abundant species in air-fed combustion, this molecule has been of specific interest for thermometry. Other diatomic molecules that may be of interest are, for example, CO, O_2, and H_2. Three-atomic molecules that might be of interest for CARS investigations in a combustion environment are H_2O and CO_2, which also have been the subject of detailed investigations (see, for example, Refs. 12 and 13).

In the present paper, results are presented of CARS investigations concerning the potential for the detection of SO_2 molecules, and the use of its spectral shape for thermometry. There are several reasons why nonintrusive measurements of SO_2 would be of major importance. First, in industrial chemical plants (for example, those producing liquid H_2SO_4), SO_2 is present in concentrations of up to 20%, and thus *in situ* measurements of temperature and/or concentration, preferably on-line, could be used for process control and steering purposes. The second reason why SO_2 is of interest—and it may be the more important one—is the role SO_2 plays as a major air pollutant. There are both direct biological effects caused by SO_2 and also indirect effects when SO_2 acts as a precursor of acidic rain by its reaction with water vapor.

The conventional technique for measurements of SO_2 is IR absorption, where normally a gas sample is extracted from the unknown gas mixture with the use of a probe. Other techniques for measurement of SO_2 based on probe sampling are conductometric and coulometric techniques. All these probe techniques have drawbacks, in so far as they are somewhat perturbing in nature, and have temporal and spatial resolution that is not always adequate. It is, in principle, possible to make an *in situ* absorption SO_2 experiment which would yield a nonperturbing measurement; however, the spatial and temporal resolution would still be low, and problems could arise in a flame environment because of spectral interferences from other flame species. Several of the problems appearing with the conventional techniques described above

Received 28 March 1988; revision received 3 June 1988.
* Author to whom correspondence should be sent.

0003-7028/88/4208-1421$2.00/0

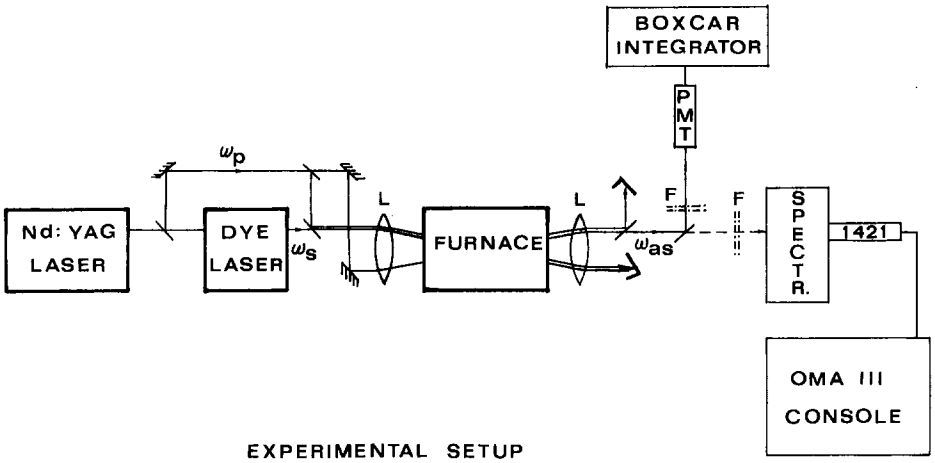

FIG. 1. Experimental setup used in the CARS experiments on SO_2.

can be avoided with the use of CARS spectroscopy, as will be described in this paper.

The chemistry of the formation of sulphur oxides is fairly straightforward,[14] and the end product is almost invariably sulphur dioxide. A comprehensive review article describing the kinetics of the combustion of sulphur compounds has been published by Cullis and Mulcahy.[15] Although the production of sulphur oxides by combustion cannot easily be controlled, there are several ways to decrease the emission of this pollutant—for example, by scrubbers or by the injection of pulverized limestone. In conjunction with these sulphur oxide trap-devices there seems to be a great interest in the possibility for on-line, nonintrusive measurements of SO_2, which could be achieved by CARS spectroscopy.

BACKGROUND

The basic theory of CARS is based on nonlinear optics and was outlined in the mid-sixties by Maker and Therune.[16] Here, we will give only a brief phenomenological description of the process. For a more detailed description we refer the reader to, for example, Refs. 1 and 17.

In a CARS experiment at least two laser beams are required (see Fig. 1), here denoted as the pump beam at ω_p and the Stokes beam at ω_s, where at least one must be tunable. By choosing the frequency difference between the two laser beams $\omega_p - \omega_s$, so that this is equal to a Raman-allowed transition, ω_R, one generates a new laser beam from the region where the two primary laser beams cross at an angle given by the phase matching condition. This new beam, the CARS beam, is generated through the third-order nonlinear susceptibility $\chi^{(3)}$. In the CARS process, one photon from the pump beam and one from the Stokes beam beat a Raman-allowed vibration, i.e., $\omega_p - \omega_s = \omega_R$. Once the vibration is excited, a second ω_p photon is scattered off, to form a blue-shifted CARS photon at $\omega_{as} = 2\omega_p - \omega_S$. The intensity I_{as} in the CARS beam is given by[1]

$$I_{as} = \left|\frac{4\pi^2\omega_{as}}{c^2}\right|^2 I_p^2 I_s |\chi^{(3)}|^2 z^2 \qquad (1)$$

where I_p and I_s are the laser intensities of the pump and Stokes beam, respectively, and z is the pathlength from which the CARS signal is generated.

The third-order susceptibility can be divided into a resonant and a nonresonant part

$$\chi = \chi_R + \chi_{NR} \qquad (2)$$

where the nonresonant part, χ_{NR}, arises from electronic and remote Raman transitions, and χ_R consists of one real and one imaginary part. For a Raman transition (j) we have

$$\chi_R = \chi' + i\chi'' = \frac{2c^4}{\hbar\omega_s^4} N\Delta_j b_j \left(\frac{d\sigma}{d\Omega}\right)_j \cdot \frac{\omega_j}{\omega_j^2 - (\omega_p - \omega_s)^2 - i\Gamma_j(\omega_p - \omega_s)} \qquad (3)$$

where $N\Delta_j$ is the population difference between the initial and final states, b_j is the line strength factor, $(\frac{d\sigma}{d\Omega})_j$ is the Raman cross section for the molecular species, and Γ_j is the Raman linewidth.

From Eqs. 1–3 it follows that a CARS spectrum has a dependence on the magnitude of χ_R and χ_{NR}, resulting in different line shapes for different concentrations of the species being studied.

Prior to running a CARS experiment, it is important to get familiar with the spectroscopy of the molecule which is to be studied. SO_2 is, strictly speaking, an asymmetric top molecule with all principal moments of inertia being different, with an O-S-O angle of 119.53°, and with an O-S distance of 1.432 Å, measured by microwave investigations.[18] However, since the two larger moments of inertia are roughly equal, the SO_2 molecule can almost be regarded as a prolate, symmetric top, which facilitates spectral identification. SO_2 has three primary vibrational-rotational bands—ν_1, ν_2, and ν_3 at 1151, 518, and 1362 cm^{-1}, respectively—in addition to several combination and overtone-bands. The infrared spectrum of SO_2 has been studied in several investigations (see, for example, Ref. 19). The Raman spectrum of SO_2 has previously been investigated theoretically and experimentally—among others, by Murphy[20] and by Brooker and Eysell,[21] who made hot-band assignment and isotopic shift mea-

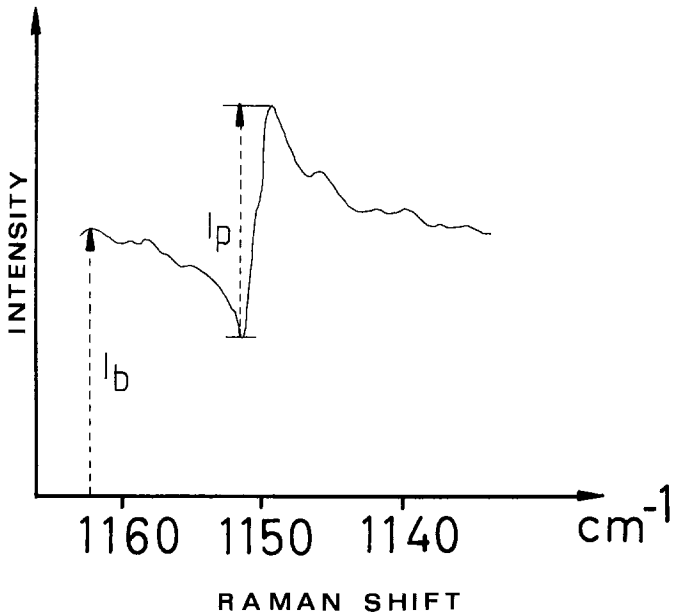

FIG. 2. SO_2 CARS spectrum from 0.2% SO_2 in N_2 at 650 Torr, 300 K. I_p and I_b are defined as shown in the figure.

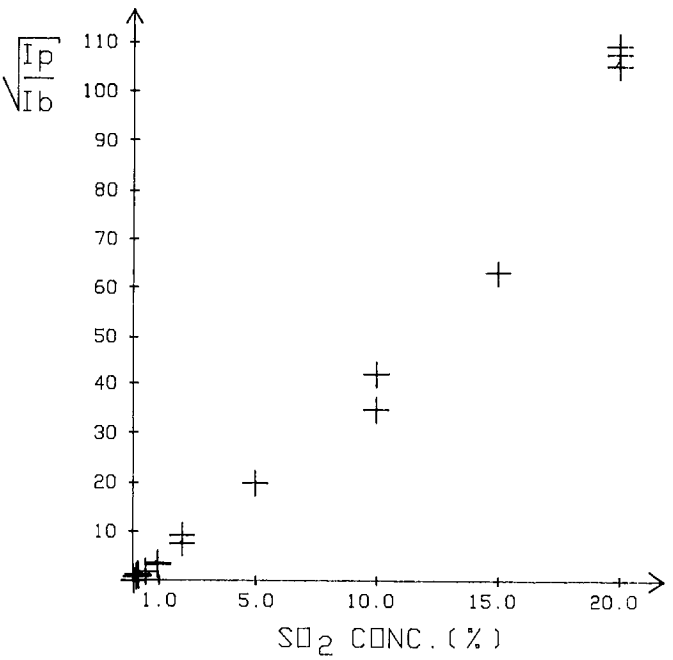

FIG. 3. $\sqrt{I_p/I_b}$ as a function of SO_2 concentration.

surements of SO_2. The Raman technique has also been used for remote detection of SO_2 using lidar techniques.[22]

In this work we have used the strongly Raman-allowed symmetric stretch, ν_1, at 1151 cm^{-1} with a Raman cross section of 5.4 times that of N_2.[1]

EXPERIMENTAL SETUP

Throughout the measurements, the planar BOXCARS technique was used and the setup can be seen in Fig. 1. A Quanta Ray DCR-1A Nd:YAG laser produced ~8 ns laser pulses of 200 mJ at 10 Hz in the frequency-doubled radiation at 532 nm. Of this radiation, 10% was split off and used as the pump beam, (ω_p) in the CARS process, while the rest was used to pump a Quanta Ray PDL-1 dye laser. Rhodamine 6G was used to produce wavelengths around 567 nm, which then served as the Stokes beam. Since this wavelength was at the edge of the dye curve, only 6–8 mJ per pulse was obtained, which, however, was quite enough in the measurements reported here. With the use of the beamsplitter (BS), the pump beam (ω_p) was split into two beams. The yellow beam (ω_s) was aligned and superimposed on one of the pump beams, with the dichroic mirror (DM). All beams were then focused in a planar BOXCAR arrangement inside a heatpipe furnace or a flame with the use of an $f = 500$ mm lens, where the crossing-angle between the laser beams was ~2°. The heat pipe was a Leybold-Heraeus, Model RoM 5/70, capable of reaching 1800 K, and the temperature was monitored with a chromel-alumel thermocouple placed inside the heatpipe. Here a quartz cell was placed, which was used to contain different SO_2/N_2 mixtures. The quartz cell limited the temperature measurements to 1200 K, as local high-temperature zones would cause cell deformation and, thus, problems in the generation of the CARS signal. Together with the created CARS beam, all laser beams were recollimated after the heatpipe, with the use of another $f = 500$ mm lens. The CARS beam was spectrally isolated from the green pump beam by two dichroic mirrors and an interference filter centered at 501 nm, corresponding to a Raman shift of 1151 cm^{-1}. In the heatpipe measurements, a photomultiplier (EMI 9558 QA) was used, and, in order to ensure a linear detector response, neutral-density filters were used to attenuate the CARS beam. The electric signal was then fed to a BOXCAR integrator, EG&G Model 4420 equipped with two Model 4422 gated integrators. The EG&G Model 4402 signal processor performed the necessary signal averaging, and the data were stored on floppy-disks for further processing. In the flame experiments the furnace was removed and SO_2 was introduced in a premixed $C_2H_2/O_2/N_2$ flame. A broad-band Stokes laser was used to permit single-shot CARS generation. As detector, an EG&G PARC OMA III unit with a 1421 detector head was used and was placed in the exit plane of a home-made 1-m spectrograph with a dispersion of ~3 Å/mm.

MEASUREMENTS AND RESULTS

In the nonflame experiments, the CARS spectra were all obtained by scanning the dye-laser wavelength. The resulting linewidth, ~0.5 cm^{-1}, of the spectra was limited by the dye laser, $\Delta\nu \simeq 0.3$ cm^{-1}, since an etalon was used in the Nd:YAG pump laser, thus reducing this linewidth to $\Delta\nu \simeq 0.15$ cm^{-1}. Normally, the wavelength of the dye laser was scanned at a rate of 0.015 cm^{-1}/s, resulting in approximately 100 laser pulses per channel in the EG&G signal processor. A typical scan of 30 cm^{-1} thus required 30 min of data acquisition.

Room-temperature Measurements. CARS measurements of SO_2 at room temperature, 300 K, posed two problems. It turned out that at this low temperature an opaque deposit was formed on the walls of the quartz cell within an hour, with the use of 200 Torr of SO_2. Also, optical breakdown was induced at a lower laser intensity than during the high-temperature measurements. However, a moderate temperature increase, 100 K, immediately eliminated both problems.

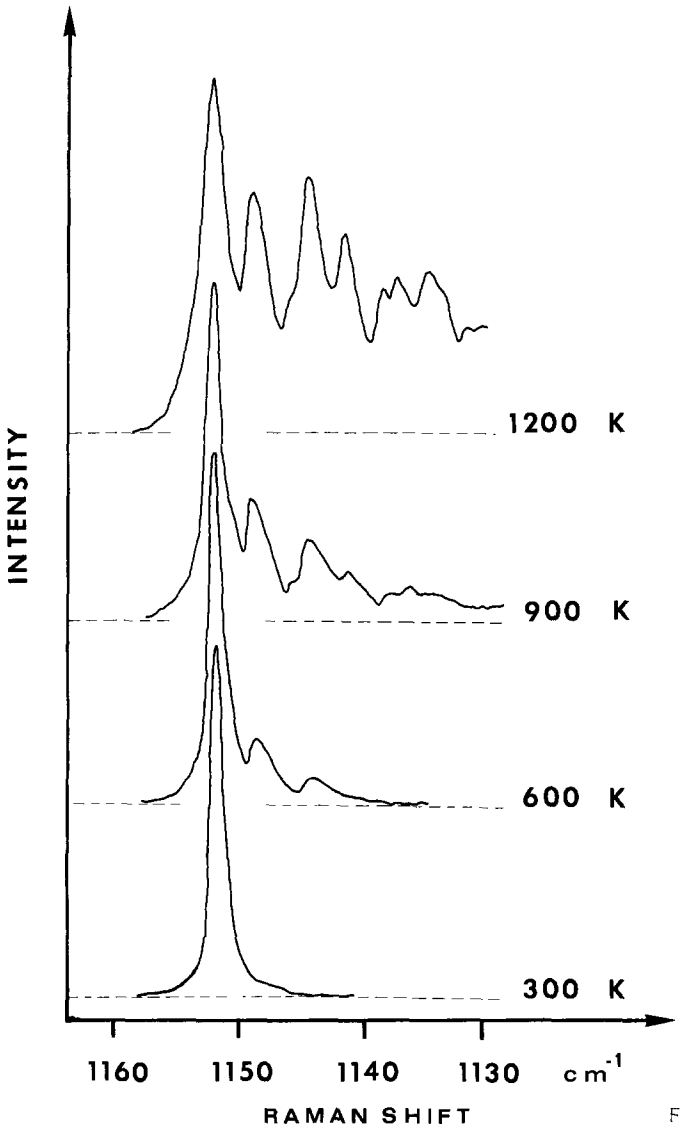

FIG. 4. SO_2 CARS spectra at different temperatures as obtained with the use of scanning CARS and a cell at elevated temperatures.

The CARS spectrum from 200 Torr of SO_2 at 300 K shows only the expected peak at 1151 cm^{-1}, and the signal was quite strong, clearly visible to the naked eye when scattered off a piece of white paper. A calibrated gas mixture of 0.2% SO_2 in nitrogen was used to estimate the detection limit. Figure 2 shows the resulting spectrum (650 Torr, 300 K). The CARS spectral shape is essentially dispersive, caused by the interference of χ_{NR} and χ_R, as described above. I_b and I_p are defined as shown in the figure, marking the background and the peak intensities of χ_{NR} and χ_R, respectively. The ratio $\sqrt{I_p/I_b}$ was measured for a number of different SO_2/N_2 mixtures on several occasions, and the results are shown in Fig. 3. As can be seen, the plot is approximately linear to 10–15% SO_2. Up to this level of SO_2 in N_2 the decrease in I_b by the replacement of N_2 by SO_2 is insignificant. However, at higher concentrations of SO_2 the background level is increasingly influenced by the dilution of N_2, and thus the values I_p/I_b are expected to change in this region, since the total pressure was kept at 650 Torr.

Measurements at Elevated Temperatures. When capturing CARS spectra of SO_2 at elevated temperatures, we used a quartz cell containing 200 Torr of SO_2. Prior to each temperature-measuring sequence, the cell was filled at 300 K and was then sealed off. In Fig. 4 the SO_2 CARS spectra at 300, 600, 900, and 1200 K can be seen. The measurements were always performed by starting at the lower temperature, since the heatpipe cooled off very slowly. By translating the thermocouple inside the cell, we found that the temperature variation along the quartz cell in the probed area was less than 5°C. From Fig. 4 it is clear that a number of additional peaks appeared when the temperature was increased. Also, the spectral widths were broadened at higher temperatures. The temperature dependence of the peak intensity was measured on several occasions over an extended period of time. The data are summarized in Fig. 5. As can be seen, the intensity varies by about a factor of 10^2 from 300 K to 1000 K, which is about the same factor as was previously found by Dreier *et al.* in measurements on N_2 and O_2.[23]

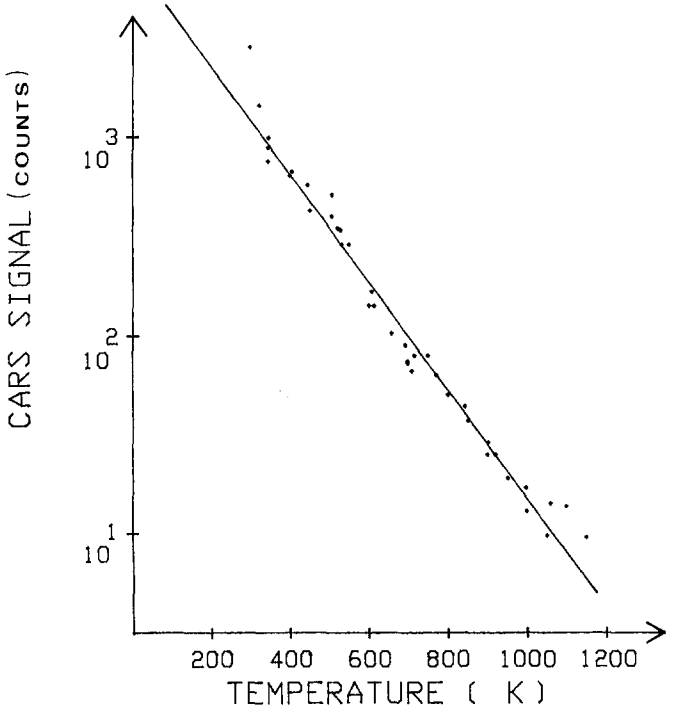

FIG. 5. Plot of the SO_2 peak CARS signal intensity at 1151 cm^{-1} as a function of temperature.

From Fig. 4 it is clear that the different peaks in the CARS spectra have different dependence on the temperature. In Fig. 6 three different ratios are plotted vs. the temperature. Again this is a compilation of data from a large number of different experimental runs. The ratios show strong temperature dependence, and the ratio (a) seems to be particularly sensitive to temperature changes within the temperature interval in question.

In order to understand the origin of the hot SO_2 CARS spectra we made preliminary attempts to identify the structures appearing at higher temperatures. In Fig. 6 the CARS spectrum at 1200 K is inserted, and the four most prominent peaks are marked with arrows. The suggested identifications are based on calculations using the expression for vibrational energy in cm^{-1} given by Shelton *et al.*:[19]

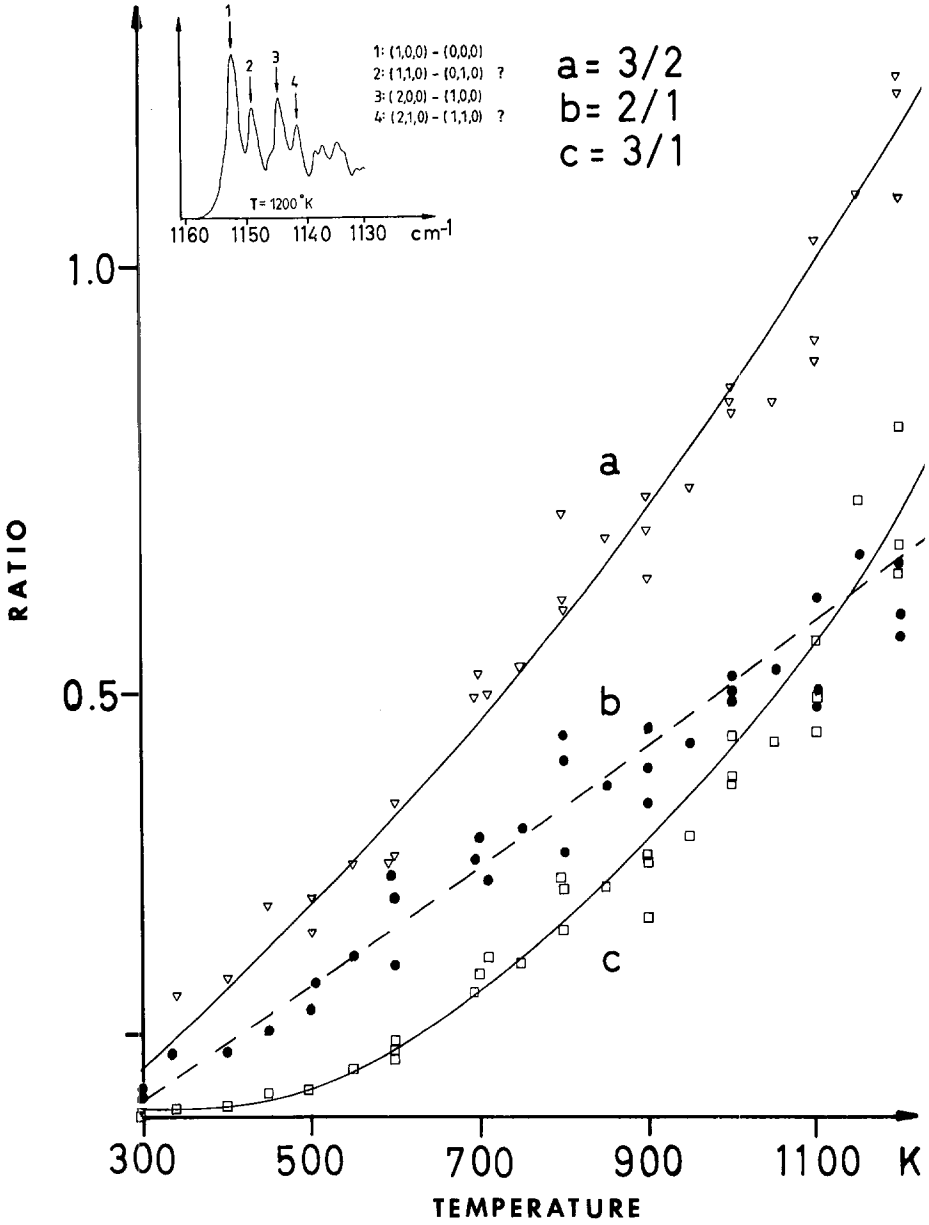

FIG. 6. Plot of different peak ratios as a function of temperature. Inserted in the figure is a spectrum at 1200 K where the different peaks are tentatively identified and labeled.

$$G(v_1, v_2, v_3) = (v_1 + \tfrac{1}{2})\omega_1 + (v_2 + \tfrac{1}{2})\omega_2 + (v_3 + \tfrac{1}{2})\omega_3 + (v_1 + \tfrac{1}{2})^2 X_{11} + (v_2 + \tfrac{1}{2})^2 X_{22} + (v_3 + \tfrac{1}{2})^2 X_{33} + (v_1 + \tfrac{1}{2})(v_2 + \tfrac{1}{2}) X_{12} + (v_1 + \tfrac{1}{2})(v_3 + \tfrac{1}{2}) X_{13} + (v_2 + \tfrac{1}{2})(v_3 + \tfrac{1}{2}) X_{23}$$

where v_1, v_2, and v_3 are the vibrational quantum numbers associated with the fundamental vibrational frequences ν_1, ν_2, and ν_3. ω_1, ω_2, and ω_3 are the zero-order harmonic frequencies, and X_{ij} are anharmonic and interaction terms. These constants are also taken from Ref. 19.

The locations of the band centers corresponding to different vibration modes are calculated to be

$$G(1,0,0)\text{–}G(0,0,0) = 1151.7 \text{ cm}^{-1}$$
$$G(2,0,0)\text{–}G(1,0,0) = 1143.8 \text{ cm}^{-1}$$
$$G(1,1,0)\text{–}G(0,1,0) = 1149.7 \text{ cm}^{-1}$$
$$G(2,1,0)\text{–}G(1,1,0) = 1141.7 \text{ cm}^{-1}$$

etc. These locations are in good agreement with the observed structure, and we conclude that the four most prominent peaks are due to the (1,0,0)–(0,0,0) and (1,1,0)–(0,1,0) transitions, together with the connected hot-bands (2,0,0)–(1,0,0) and (2,1,0)–(1,1,0).

Since it was not possible to go to higher temperatures in the heatpipe because of cell deformations starting at 1200 K, concluding measurements were performed that aimed at recording CARS spectra from SO_2 in a flame. Because of possible corrosion problems in the burner, as well as unwanted chemical reactions, SO_2 was not introduced in the premixed burner together with the fuel and oxidant. Instead, SO_2 was introduced in the post-flame region by a copper probe, which was not nonintrusive but gave a good possibility of allowing the study of the CARS spectrum from SO_2 at flame temperatures.

In Fig. 7 the SO_2 CARS spectrum is shown as obtained when corrected for the broad-band dye laser distribution.

As can be seen, the spectrum is now considerably broader than it is in the cell experiment, extending over ~150 cm^{-1}. The drop in intensity around 1000 cm^{-1} is caused by the limited photo-sensitive area of the diode array. The spectrum shows several bands. However, no attempts have been made to analyze their origin. The temperature in the flame was not explicitly measured, but previous CARS experiments on this burner with the same gas flows and N_2 as the test species have given a temperature around 2000 K. It is difficult to compare the spectrum in Fig. 7 with those in Fig. 4, since the spectral resolution is different and because the temperature and concentration of SO_2 are not exactly known at the measuring point. However, by looking at the spectra in Fig. 4 and the strong temperature dependence of the spectral change, one could anticipate a very broad flame spectrum.

Since the SO_2 was introduced in the post-flame region and since the conversion into other sulphur-containing molecules is expected to be rather weak,[24] one should not normally expect any spectral interference from these species. The species that might interfere is SO, which has a Raman shift interfering with that from SO_2 (SO, 1150 cm^{-1}; SO_2, 1151 cm^{-1}).[1] However, even under extreme conditions SO has a concentration about an order of magnitude lower than SO_2,[24] which, with the quadratic concentration dependence on the CARS signal, would strongly reduce interference even from SO.

DISCUSSION AND CONCLUSIONS

As has been demonstrated in this paper, CARS spectroscopy has a considerable potential for the detection of low concentrations of SO_2. In addition, the possibilities of using this species for temperature measurements also seem attractive. According to Fig. 4, the spectral changes from room temperature to 1200 K are considerable. This result should be compared to the temperature dependence of the N_2 CARS spectra, where the intensity of the hot-band transition, $v = 1 \rightarrow v = 2$, is barely seen below 1000 K (<5% of the fundamental band $v = 0 \rightarrow v = 1$). The temperature change in this case is, rather, seen as a broadening of the fundamental band, due to the increased population of higher rotational levels.

In this study the temperature dependence of the SO_2 CARS spectra was examined with no background, χ_{NR}. However, in a measuring situation of an unknown composition the nonresonant background may change the calibration curves shown in Fig. 6. Clearly in this situation there might be a need for a model generating theoretical CARS spectra of SO_2 with χ_{NR} and T as parameters, as in the case of most diatomic and some polyatomic molecules. To our knowledge no such model has been presented for SO_2. In addition to the problem that SO_2 is actually an asymmetric molecule, problems would arise due to lack of fundamental data, for example, for Raman linewidths. An alternative to this procedure could be to extend the measurement presented in this study to also include measurements at varying temperatures and concentrations, and in this way to build up a library of CARS spectra which could be of use in a real measurement situation. A third method, and probably the best one, is to use an experimental approach where the nonresonant background is rejected by using different polarization orientations of the laser beams in combination with a polarizer in the CARS beam.[25]

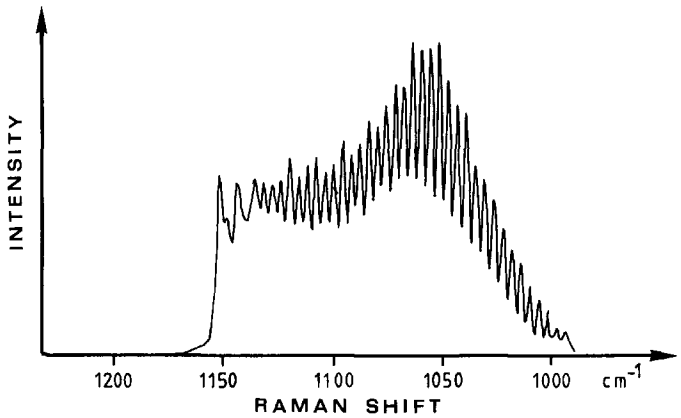

FIG. 7. SO_2 CARS spectrum from a SO_2^- doped $C_2H_2/O_2/N_2$ flame.

Concerning the high-temperature measurements of SO_2, it is worth mentioning the quite drastic spectral changes at elevated temperatures, which have previously been seen both in the UV region (see, for example, Ref. 26) and in the infrared[27] and which are suggested to be the reversible formation of an isomer.[28] The structure of this isomer is not known exactly, but it has been suggested that the bond angle is more acute than it is in normal SO_2 and that the bond lengths are longer.[29] As was pointed out in Ref. 15, the question of an isomer is not only an academic one, since this factor would strongly influence the equilibrium composition of flame gases containing sulfur. Although there has been strong indication of the formation of an isomer of SO_2 at high temperature, other explanations for the spectral behavior at higher temperatures have also been put forward.[30] In our study we have not tried to contribute to this discussion, since our temperature range was limited to very hot gases (~2000 K) and gases with relatively low temperature (<1200 K).

ACKNOWLEDGMENTS

The authors gratefully acknowledge stimulating discussions with Stefan Kröll, and the constant support from Sune Svanberg. We are also very thankful to Per-Erik Bengtsson and Christer Löfström for their help in performing the flame measurements. This work was financially supported by Boliden AB and the Swedish Board for Technical Developments (STU).

1. A. C. Eckbreth, P. A. Bonczyk, and J. F. Verdieck, Prog. in Energy and Comb. Sci. **5**, 253 (1979).
2. *Laser Probes for Combustion Chemistry*, D. R. Crosley, Ed. (American Chemical Society, Washington, D.C., 1980).
3. M. Aldén, *Applications of Laser Techniques for Combustion Studies*, Ph.D. Thesis, Lund Report of Atomic Physics LRAP-22, Lund Institute of Technology, Lund, Sweden (1983).
4. P. R. Regnier and J. P. E. Taran, Appl. Phys. Lett. **23**, 240 (1973).
5. P. R. Regnier, F. Moya, and J. P. E. Taran, AIAAJ. **12**, 826 (1974).
6. W. B. Roh, P. W. Schreiber, and J. P. E. Taran, Appl. Phys. Lett. **29**, 174 (1976).
7. A. C. Eckbreth, Appl. Phys. Lett. **32**, 421 (1978).
8. A. C. Eckbreth, Comb. and Flame **39**, 133 (1980).
9. D. Klick, K. A. Marko, and L. Rimai, Appl. Opt. **20**, 1178 (1981).
10. M. Aldén and S. Wallin, Appl. Opt. **24**, 3434 (1985).
11. E. J. Beiting, Appl. Opt. **25**, 1684 (1986).
12. R. J. Hall and J. A. Shirley, Appl. Spectrosc. **37**, 196 (1983).
13. N. Papineau and M. Péalat, Appl. Opt. **24**, 3002 (1985).

14. R. A. Strehlow, *Combustion Fundamentals* (McGraw-Hill, New York, 1985).
15. C. F. Cullis and M. F. R. Mulcahy, Comb. and Flame **18,** 222 (1972).
16. P. D. Maker and R. W. Terhune, Phys. Rev. **137,** A801 (1985).
17. S. Druet and J. P. Taran, Prog. Quant. Electr. **7,** 1 (1981).
18. M. H. Sirretz, J. Chem. Phys. **19,** 938 (1951).
19. R. D. Shelton, A. H. Nielsen, and W. H. Fletcher, J. Chem. Phys. **21,** 2178 (1953).
20. W. A. Murphy, J. Raman Spectrosc. **11,** 339 (1981).
21. M. H. Brooker and H. H. Eysell, J. Raman Spectrosc. **11,** 322 (1981).
22. T. Hirschfeld, E. R. Schildkvant, H. Tannenbaum, and D. Tannenbaum, Appl. Phys. Lett. **22,** 38 (1973).
23. T. Dreier, B. Lange, J. Wolfrum, and M. Zahn, Appl. Phys. **B45,** 183 (1988).
24. G. M. Johnson, C. J. Mattews, M. Y. Smith, and D. J. Williams, Combust. and Flame **15,** 211 (1970).
25. L. A. Rahn, L. J. Zych, and P. L. Mattern, Opt. Comm. **30,** 249 (1979).
26. H. A. Olschewski, J. Troe, and H. G. Wagner, Z. Physics Chem. **44,** 173 (1965).
27. P. A. Giguére and R. Savoie, Can. J. Chem. **43,** 2357 (1965).
28. J. J. McCarrey and W. D. McGrath, Proc. Roy. Soc. (London) **A278,** 490 (1964).
29. E. F. Hayis and G. V. Pfeiffer, Am. Chem. Soc. **90,** 4773 (1968).
30. N. Basco and R. D. Morsi, Proc. Roy. Soc. (London) **A321,** 129 (1971).

A Monte Carlo Study of the Effect of Noise on Wavelength Selection During Computerized Wavelength Searches

HOWARD MARK

Bran and Luebbe Analyzing Technologies, 103 Fairview Industrial Park, Elmsford, New York 10523

The process of selecting wavelengths for performing quantitative analysis in the near-infrared is notorious for its instability. A Monte Carlo technique was used to investigate the sensitivity of the wavelength selection process to the noise content of the spectra. The random nature of the noise causes the wavelengths to be selected at random; this seems to be sufficient to explain the instability of the selection process. The statistics of the selection process are insensitive to error in the dependent variable, and, within limits, also insensitive to the amount of noise in the spectral data. The statistics are sensitive to the number of samples in the data set and to the nature of the distribution of the noise.

Index Headings: **Computer applications; Reflectance spectroscopy; NIR analysis; Chemometrics; Calibration techniques.**

INTRODUCTION

It has been many years since the initial development of the spectroscopic technique now called Near Infrared Reflectance Analysis (NIRA).[1] In all that time, one of the most intractable problems in the use of this analytical technology has revolved around the question of developing a methodology for selecting the wavelengths to use for a given analysis.

In practice, many empirical methods have been developed for selecting the analytical wavelengths (see the discussion in Ref. 2 for an excellent review of the techniques currently in use). However, most of these methods are subject to a certain difficulty. This difficulty arises because an automatic computerized wavelength selection technique is almost invariably included in the method development process.

There are a number of excellent reasons for this, among them the fact that many of the analyses of interest are for powdered solid materials. Data from such specimens show an effect variously called the "particle size effect" or the "repack effect." This phenomenon causes repeat readings of the same aliquot of the specimen—if dumped out of and then repacked into the sample holder—to show an offset which is systematic across the wavelengths but random in direction and magnitude from pack to pack.[3] Clearly, a measurement at *some* wavelength is needed to account for this extraneous variation of the spectral data, but just as clearly, "particle size effect" does not have a characteristic absorbance band, such as chemical constituents possess. Furthermore, many of the constituents in natural products, where this technology has its most widespread use, have at least some absorbance at virtually every wavelength in the near-infrared region. In many cases the desired analysis is for some characteristic of the sample defined by the process, such as "baking quality," where the chemistry and spectroscopy of the analysis are ill-defined or unknown.

For all these reasons, automatic wavelength searches are used. One chooses the "best" wavelength so as to optimize the calibration by finding the wavelengths where one of the calibration statistics shows the calibration to be best. This optimum value could be either a maximum or a minimum value, depending upon the statistic used: if correlation coefficient, for example, is the chosen statistic, it would be maximized, while if Standard Error of Estimate (SEE) is the test statistic, it would be minimized.

The difficulty that arises when automatic wavelength selection methods are used is that, when such an experiment is done more than once (i.e., with a set of data from similar but not identical samples), the wavelengths that are chosen are rarely the same in the different experiments. Furthermore, the interactive nature of the data at different wavelengths in the NIR spectra causes large shifts in all the wavelengths that are chosen by such searches.

Currently there is a trend toward use of calibration methods, such as Principal Component Analysis (PCA) and Partial Least-Squares (PLS), that do not require wavelength selection because data at all available wavelengths are used. However, this is not a complete solution to the problem either. Not only are there already a large

Received 25 April 1988; revision received 8 June 1988.

0003-7028/88/4208-1427$2.00/0